Supplementary Methods

Treatment with agonists and antagonists

RXR agonists and antagonists were used in BMMs. The agonist 9cRA was used at 1μM and antagonist HX531 at 10μM (Sigma) from DMSO stock concentrations. The corresponding amount of DMSO was added to control samples. The concentration for HX531 was chosen based on previous studies (Yamauchi et al., 2001).

In Situ Hybridization

The PLP probe was denatured for 10min at 75°C then added to spinal cord sections. Slides were coverslipped and incubated in a chamber with 50% formamide and SSC in diethylpyrocarbonate-treated dH_2O and hybridized overnight at 65°C. Slides were then incubated in wash buffer (1× SSC, 50% formamide, 0.1% Tween-20) at 65°C for 15min. Slides were washed in MABT (100mM maleic acid, 150mM NaCl, 0.1%Tween-20, pH 7.5) and incubated in blocking solution (2% blocking, 10% heat-inactivated sheep serum in MABT) for 1h. Anti-digoxygenin-AP fragments (Roche, 1:1500) in blocking solution were added to slides, and slides were incubated overnight at 4°C. Slides were then washed in MABT and twice in staining buffer (100mM Tris-HCl, 100mM NaCl, 5mM $MgCl_2$, pH 9) followed by incubation in BCIP/NBT stock solution (Roche) at 37°C for 1-2h. Slides were coverslipped with Aquamount and visualized in brightfield with a Nikon Eclipse E600 microscope.

Electron Microscopy

Glutaraldehyde-perfused spinal cords were post-fixed in 2% osmium tetroxide (Oxkem Ltd) in phosphate buffer at 4°C overnight followed by dehydration in 70%, 95%, and 100% ethanol. Tissue was put in propylene oxide then left in 50% propylene oxide, 50% resin mix (TAAB) for 3h and transferred to 100% resin mix overnight. Embedding capsules were incubated at 60°C for 12-24h. Embedded samples were cut in 90 nm sections on an ultramicrotome (Reichert Ultracut E) and visualized using a Transmission Electron Microscope (Hitachi H600). Films (Kodak) were developed and scanned at high resolution and analyzed with ImageJ.

Microarrays & Ingenuity Pathway Analysis

Total RNA was labeled for use with the Affymetrix Human Gene 1.0 ST Array (Affymetrix, Inc). Labeled cRNA was hybridized to these arrays in blinded fashion. The Affymetrix scanner 3000 was used in conjunction with Affymetrix GeneChip Operation Software to generate one .CEL file per hybridized cRNA. These files are in NCBI GEO for download (GSE66988). The Affymetrix

Expression Console was next used to summarize the data contained across all .CEL files and generate 33,297 RMA normalized gene fragment expression values per file. Quality of the resulting values was challenged and assured via Tukey box plot, covariance-based PCA, and correlation-based heat map using functions supported in "R". Lowess modeling of the data was performed to characterize noise for the system and discard gene fragments having noise-biased data (all RMA expression values < 7). For gene fragments not discarded, differential expression across sample classes was tested for via ANOVA under FDR MCC condition. Gene fragments having a corrected $p<0.05$ by this test were subset and post hoc analysis performed using the TukeyHSD test. Ingenuity Pathway Analysis software was used to create diagrams for comparing biological pathways and determining canonical pathways

Ingenuity Pathway Analysis "Core Analysis" was performed on the gene fragments having a corrected $p<0.05$ in both young and old monocytes to determine the canonical pathways significantly affected by myelin debris phagocytosis using a right-tailed Fisher Exact Test. The software determines these significant pathways based on the 1) known list of genes in that pathway, 2) the total number of genes in our platform, and 3) the number of significantly altered genes in both our dataset and a given pathway. These results showed that canonical pathways involving RXR and several different binding partners are differentially regulated upon myelin phagocytosis in young (≤35 years old) and old (≥55 years old) human monocytes compared to resting cells. *$p<0.05$ for the genes differentially regulated in the given pathway.

PCR Arrays and qPCR

Isolated RNA was converted to cDNA using the QuantiTect Reverse Transcription Kit (Qiagen). cDNA was pooled from 6 samples in each group and added to SYBR Green qPCR SuperMix (Bio-Rad). Each sample was aliquoted on the Human Retinoic Acid Signaling PCR Array (SABiosciences), with primer pairs for 84 genes in the RXR pathway. Plates were run on a CFX96 Detection System (Bio-Rad). Data normalization was performed using Excel 2010. Relative quantification was used to compare samples to untreated, Young (≤35 years old) controls, resulting in ΔCt values used to calculate relative fold changes. The genes significantly affected by bexarotene treatment ($|FC| > 1.5$) were plotted.

M1/M2 Human Macrophages

Monocytes were isolated and plated at $1x10^6$/well in 12-well plates. All cells were plated in 1 ml media/well. Media and protocol were adapted from (Mia et al., 2014). Basic media was composed of RPMI 1640, 10% FBS, 100 u/ml Pen/Strep, and 20 μM β-mercaptoethanol. For M1-polarised cells,

50 ng/ml GM-CSF was added to media. For M2-polarised cells, 50 ng/ml M-CSF was added to media. On Day 6, cells were further polarised to M1 and M2 phenotypes. M1 cells were plated in basic media plus: 20 ng/ml IFNγ, 20 ng/ml TNFα, and 50 ng/ml LPS (Peprotech). M2 cells were plated in basic media plus: 20 ng/ml IL-4 and 20 ng/ml IL-10 (Peprotech). After 24 hours of polarisation, cells were collected and analysed by FACS. Cells were resuspended in X-vivo without phenol red and $1x10^5$ cells/treatment group were stained with M1 and M2 markers for 15 min at 37°C in a 96-well plate. CD80 was used as an M1 marker, and CD163 was used as an M2 marker. For all macrophages, CD11b was used. After staining, 10 μg/ml pHrodo labelled myelin was added to phagocytosing groups for 20 min at 37°C. Cells were washed with FACS buffer and fixed using BD FACS Cytofix buffer (100 μl/well) for 20 min at 4°C. Plates were centrifuged at 250 *g* at 4°C for 5min. Then, cells were resuspended in FACS 1X Perm/Wash Buffer (BD) and centrifuged as before. Cells were finally resuspended in 150 μl FACS buffer/well and run on a BD LSR II flow cytometer using BD FACSDiva 6.1 Software. Mean fluorescence intensity for all markers was determined by dividing the MFI of each phagocytosing group to the MFI of the control, resting macrophages.

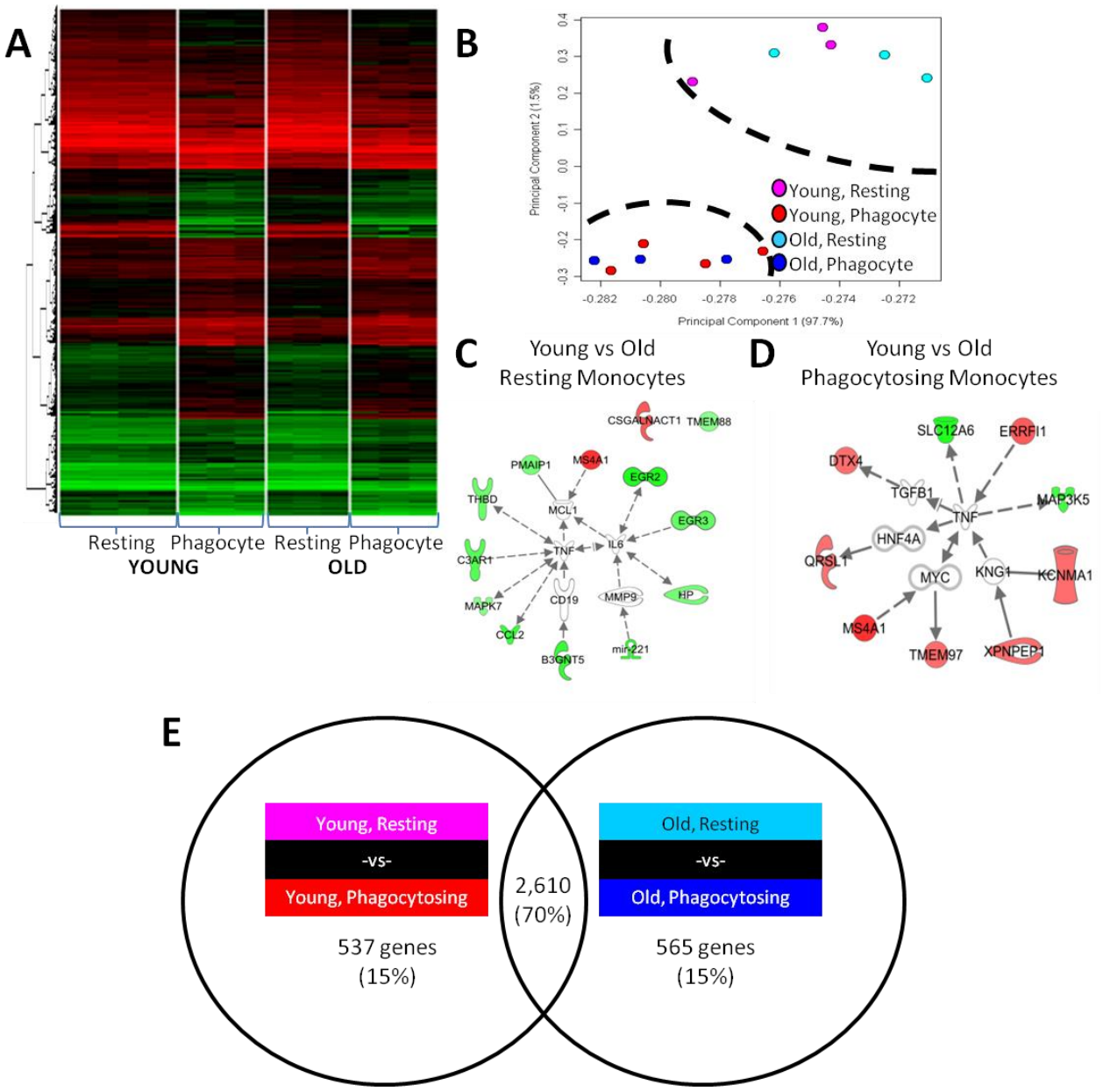

Supplementary Figure 1. Microarrays display independent clustering of phagocytosing and resting cells, with phagocytosis causing differential gene expression in young and aged monocytes. (A-B) Heat map and principal component analysis of young resting, young phagocytosing, old resting, and old phagocytosing monocytes. Phagocytosis has a greater effect on gene expression than age alone. (C) After noise filtering and stringent analysis, only 13 genes, mainly related to inflammation in macrophages, were significantly different in old resting compared to young resting monocytes, and (D) only 9 genes were significantly different in old phagocytosing compared to young phagocytosing monocytes. (E) Venn diagram comparing the unique genes changed upon phagocytosis in young cells (537 genes) versus those changed in old (565 genes) reveals that 30% of the genes changing in response to myelin exposure are differentially regulated due to age. Two-way ANOVA under FDR MCC and posthoc Tukey's HSD test. n=3/group. Red=downregulated, Green=upregulated.

RXR-related Pathway Affected	# Genes in Pathway ↑ in Young	# Genes in Pathway ↓ in Young	# Genes in Pathway ↑ in Old	# Genes in Pathway ↓ in Old
RAR/RXR Activation	N/A	N/A	2*	5*
PPARα/RXR Activation	6*	2*	3*	2*
LXR/RXR Activation	4*	1*	3*	1*
PXR/RXR Activation	1	2	1	2
TR/RXR Activation	2	1	1	3
FXR/RXR Activation	2	1	N/A	N/A
CAR/RXR Activation	N/A	N/A	0	1
LPS Inhibition of RXR	-3*	-1*	-5*	-2*
VDR/RXR Activation	1	1	0	2
TOTAL	**13**	**7**	**5**	**14**

Supplementary Table 1. Independent genes in several RXR-related canonical pathways are more significantly downregulated in aged myelin-phagocytosing monocytes and upregulated in young cells.

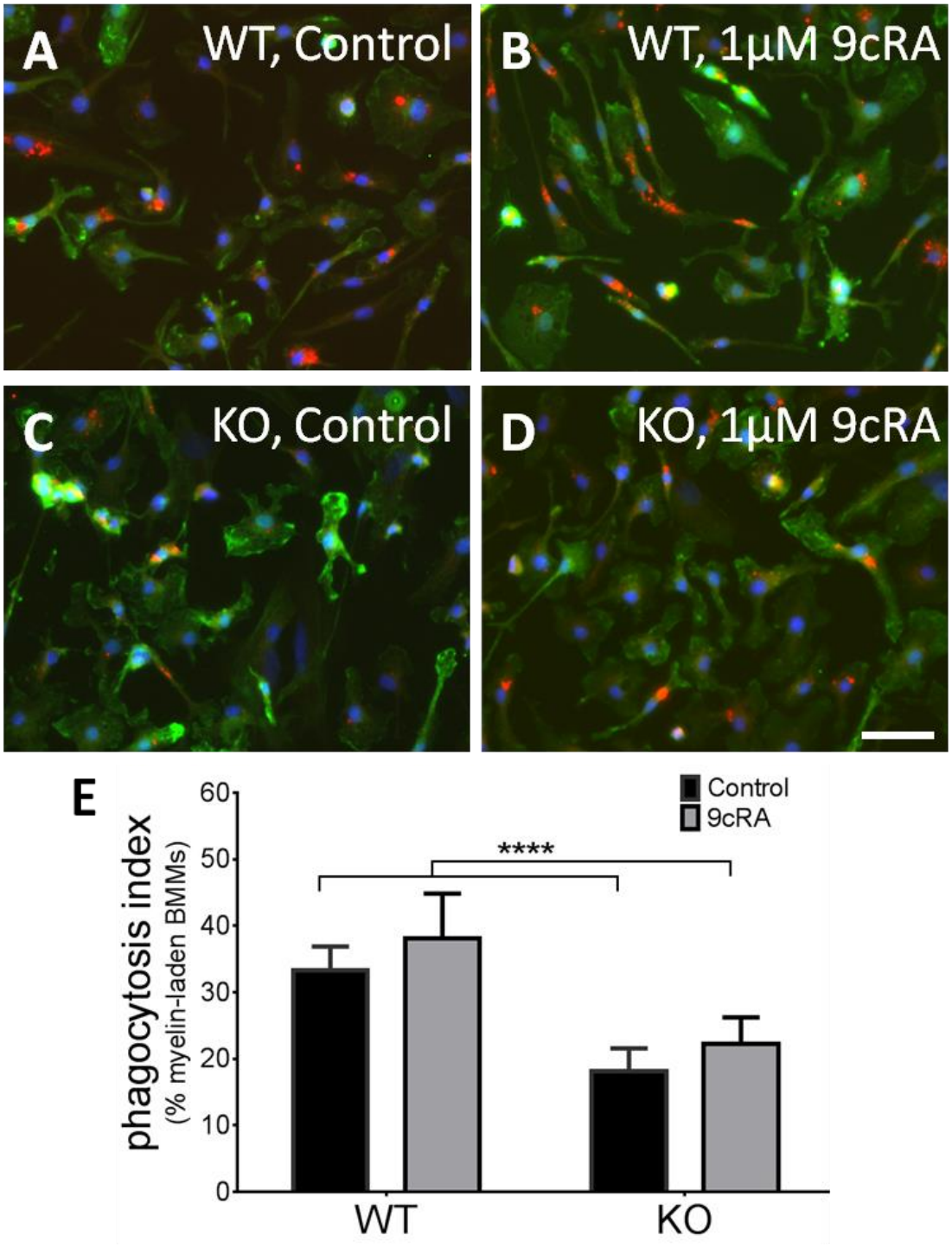

Supplementary Figure 2. Macrophages from RXRα KO mice display significantly reduced myelin debris phagocytosis. (A-B) BMMs from WT mice are able to phagocytose myelin debris, both before (A, 33.3±3.5%) and after treatment with 9cRA (B, 38.1±6%). (C-D) However, only 18.1% (±3.5%) of KO macrophages consumed debris. KO macrophages, like WT, displayed a slight but not significant increase in phagocytosis upon 9cRA treatment (D, 22.3±3.9%). (E) Overall, WT BMMs phagocytosed more myelin debris than KOs. Phagocytosis index = (%Myelin+Iba+ cells). Scale bar = 50μm. Two-way ANOVA and posthoc Sidak's test, ****$p<0.0001$, n=4/group.

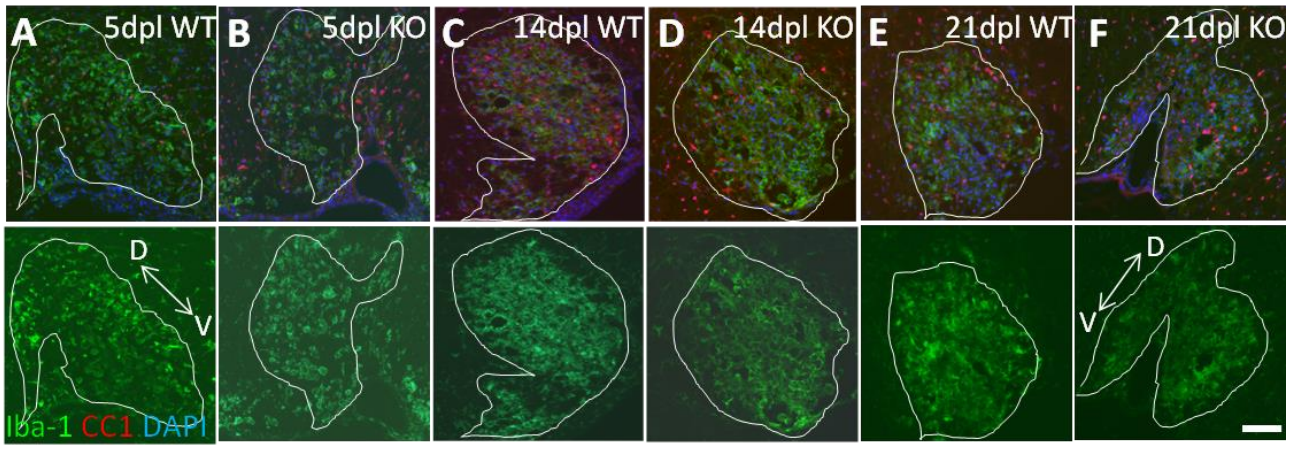

Supplementary Figure 3. Macrophages invade the demyelinated lesion of both WT and KO RXRα mice. Lysolecithin-induced demyelinated lesion is denoted by DAPI-labelling (white outline), and Iba1 was used to label blood-derived macrophages and microglia. (A-B) At 5dpl, phagocytes are active in the lesions of both WT and KO mice and many appear to have an amoeboid shape throughout the lesion. (C-F) In both WT and KO lesions, a prominent macrophage response is evident at 14dpl and 21dpl as well; however, Iba1 was visualised with more diffuse staining throughout the lesion, providing effective demarcation of the lesion but was difficult to quantify, with almost all DAPI-labelled cells also Iba1+. D↔V represents Dorsal↔Ventral axis.

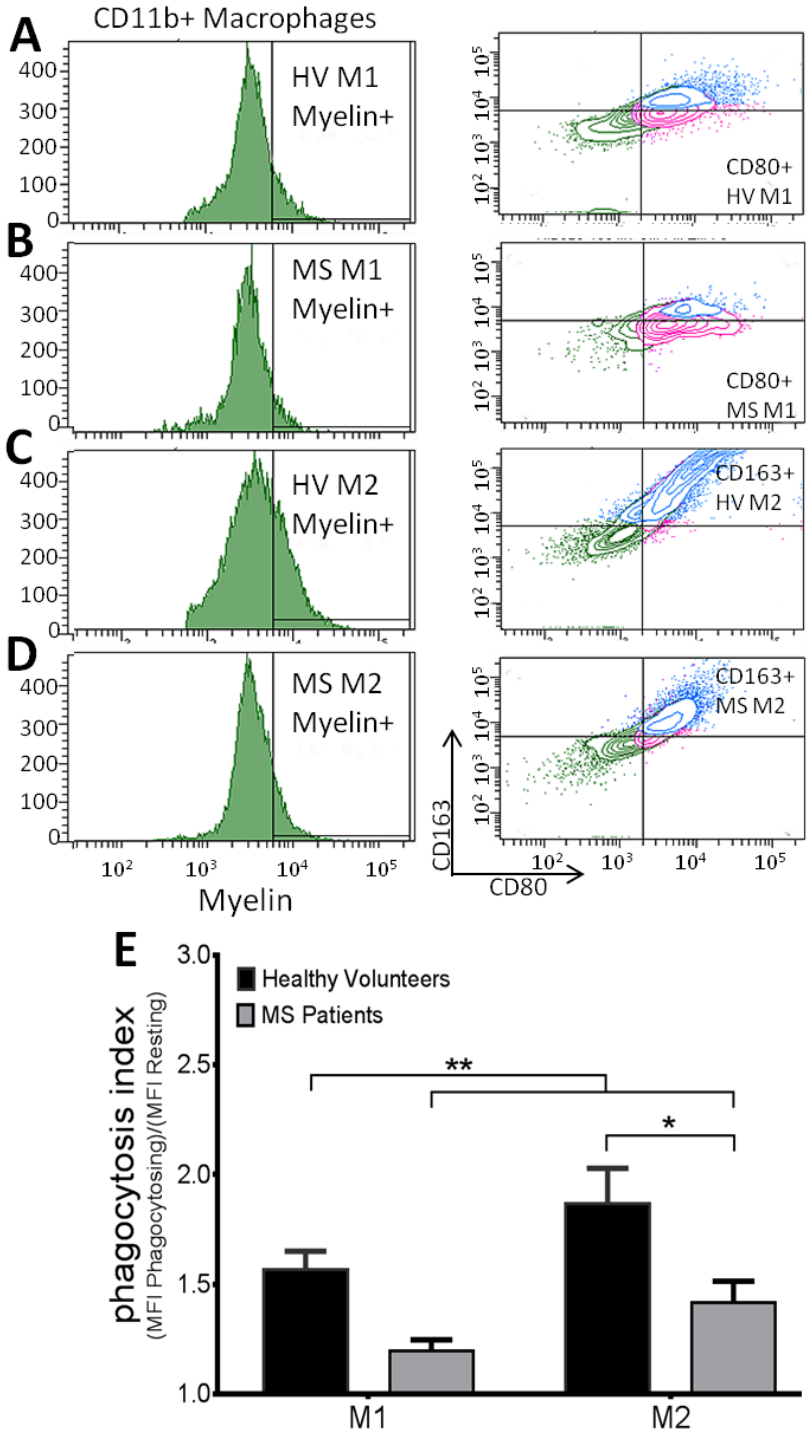

Supplementary Figure 4. Human M1 and M2 macrophages from multiple sclerosis patients display reduced myelin debris phagocytosis. Monocytes from multiple sclerosis patients were differentiated *in vitro* to determine if disease state also affects phagocytosis in human macrophages. (A-B) M1-polarised macrophages from HVs (A) show a trend towards increased myelin debris phagocytosis compared to those from MS patients (B). Flow cytometry confirmed that M1 cells express the inflammatory marker CD80. (C-D) M2 macrophages from HVs (C) phagocytose significantly more myelin debris than M2-polarised cells from MS patients (D). CD163 is highly expressed in M2 cells. (E) Overall, polarised macrophages from MS patients display reduced phagocytic capacity, and M2-polarised macrophages from both HVs and MS patients phagocytose more myelin debris than M1. Phagocytosis index = (MFI myelin-phagocytosing macrophages/ MFI resting macrophages). Two-way ANOVA and posthoc Sidak's test, *$p<0.05$, **$p<0.01$, n=10/group.

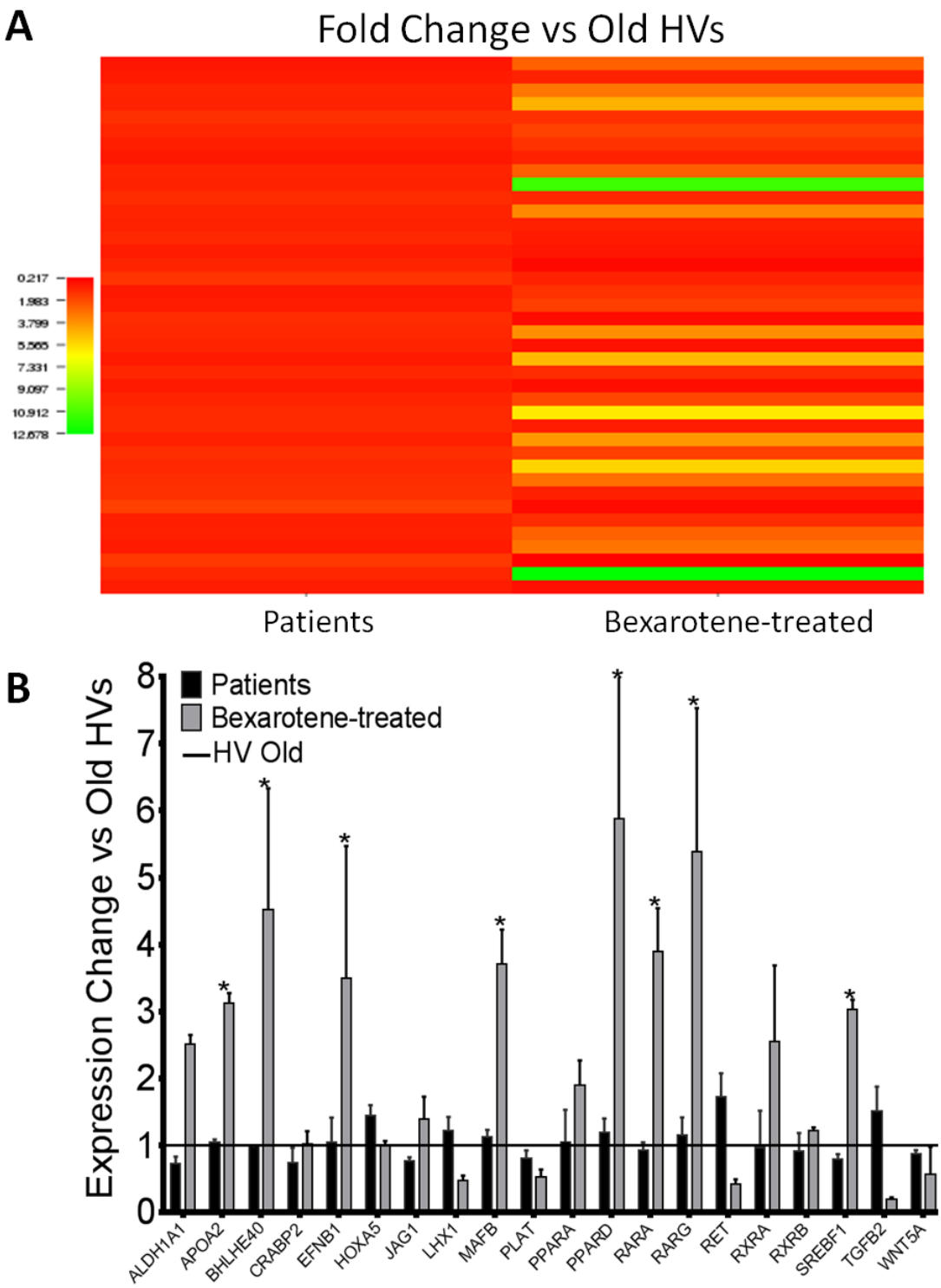

Supplementary Figure 5. RXR signaling is similar in myelin-phagocytosing multiple sclerosis patient monocytes and old HV monocytes. RXR signaling qPCR arrays were performed on myelin-phagocytosing monocytes from Old HVs, multiple sclerosis patients, and bexarotene-treated patient cells, and relative fold changes were calculated compared to myelin-phagocytosing old HVs. (A) Heat map of RXR-related genes shows that there is similarity in RXR signaling between Old HVs and patient cells, with changes upon bexarotene treatment of patient cells. (B) Several RXR-related genes showed a difference in fold change compared to old HVs in bexarotene-treated patient monocytes, with fewer differences seen in untreated patient cells. Two-way ANOVA and posthoc Bonferroni's correction, *$p<0.05$, n=6/group.

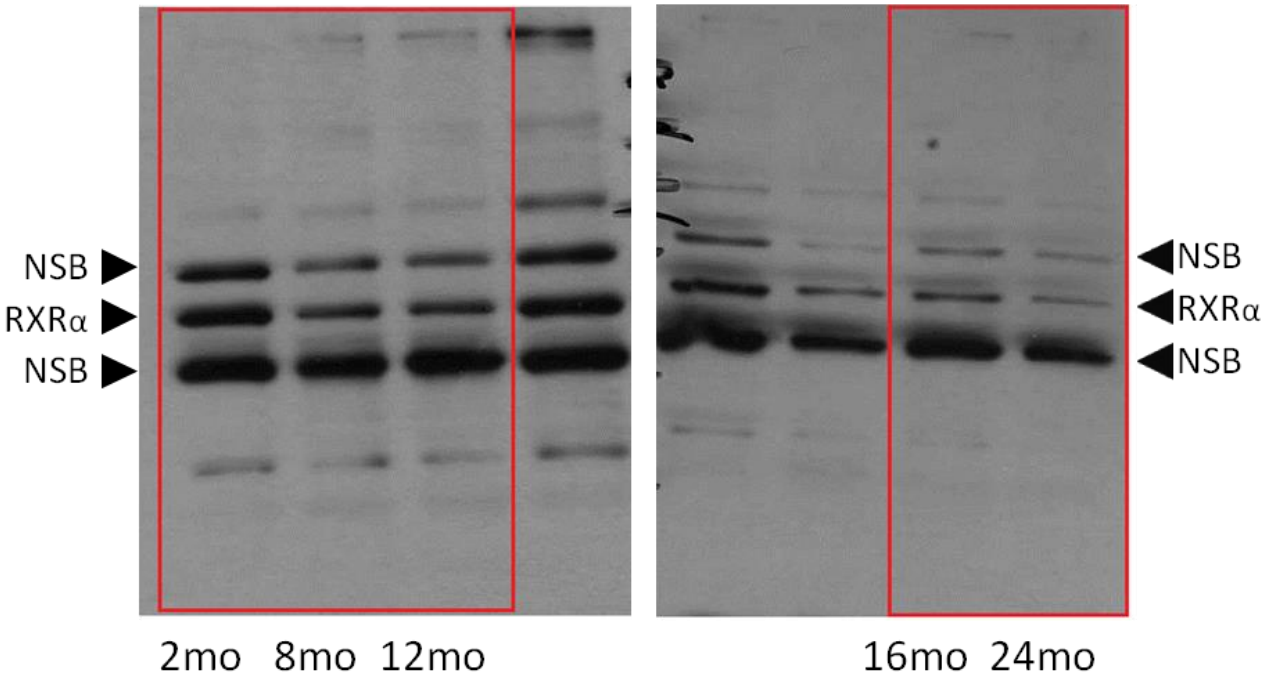

Supplementary Figure 6. Full gels for RXRα expression in ageing BMMs (Fig. 3). RXRα band of interest is highlighted to the left at 55kd with the non-specific bands labeled as NSB above and below the band of interest. These NSBs have previously been reported using the same antibody (Kuhla et al., 2011, Menéndez-Gutiérrez et al., 2015). Age of mouse BMM is listed under the gel and bands used in the paper are highlighted by a red box.